JACS
JOURNAL OF THE AMERICAN CHEMICAL SOCIETY

Article

pubs.acs.org/JACS

Light-Responsive and pH-Responsive DNA Microcapsules for Controlled Release of Loads

Fujian Huang,[†] Wei-Ching Liao,[†] Yang Sung Sohn,[‡] Rachel Nechushtai,[‡] Chun-Hua Lu,[†] and Itamar Willner*,[†]

[†]Institute of Chemistry, Center for Nanoscience and Nanotechnology, The Hebrew University of Jerusalem, Jerusalem 91904, Israel

[‡]Institute of Life Sciences, The Hebrew University of Jerusalem, Jerusalem 91904, Israel

S *Supporting Information*

ABSTRACT: A method to assemble light-responsive or pH-responsive microcapsules loaded with different loads (tetramethylrhodamine-modified dextran, TMR-D; microperoxidase-11, MP-11; CdSe/ZnS quantum dots; or doxorubicin-modified dextran, DOX-D) is described. The method is based on the layer-by-layer deposition of sequence-specific nucleic acids on poly(allylamine hydrochloride)-functionalized $CaCO_3$ core microparticles, loaded with the different loads, that after the dissolution of the core particles with EDTA yields the stimuli-responsive microcapsules that include the respective loads. The light-responsive microcapsules are composed of photocleavable o-nitrobenzyl-phosphate-modified DNA shells, and the pH-responsive microcapsules are made of a cytosine-rich layer cross-linked by nucleic acid bridges. Irradiating the o-nitrobenzyl phosphate-functionalized microcapsules, λ = 365 nm, or subjecting the pH-responsive microcapsules to pH = 5.0, results in the cleavage of the microcapsule shells and the release of the loads. Preliminary studies address the cytotoxicity of the DOX-D-loaded microcapsules toward MDA-MB-231 breast cancer cells and normal MCF-10A breast epithelial cells. Selective cytotoxicity of the DOX-D-loaded microcapsules toward cancer cells is demonstrated.

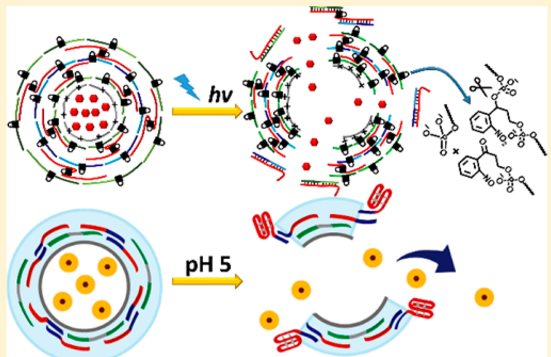

INTRODUCTION

The fabrication of microcapsules by layer-by-layer deposition processes and the encapsulation of macromolecular loads in the microcapsules attract substantial research efforts directed to the implementation of these systems as microcarriers for controlled release.[1−5] One method to prepare substrate-loaded microcapsules involves the coprecipitation of macromolecular loads with $CaCO_3$ microparticles acting as core-templates for coating by polymer shells.[6,7] The subsequent dissolution of the $CaCO_3$ core yields, then, the substrate-loaded microcapsules. Different methods to assemble the shells of the microcapsules were reported,[8−14] and a variety of external stimuli to degrade the microcapsules and release the loads were discussed. These included the thermal degradation of the microcapsules by the light-induced excitation of plasmonic nanoparticles entrapped in the microcapsules,[15−17] by the local heating of magnetic nanoparticle-loaded microcapsules using an alternate magnetic field,[18] and by the mechanical ultrasound or microwave agitation of the microcapsules.[19−22] Also, chemical triggers such as pH,[23] salts,[24] gases,[25] carbohydrates,[26] disulfide-bond reducing agents,[27] and enzymes[28,29] were used to degrade the microcapsules and to release the encapsulated loads. Different applications of substrate-loaded microcapsules were suggested, including biomedical uses as drug-carrier for controlled release[30−32] and imaging agents,[33] for sensing,[34,35] and as functional microreservoirs for reactions.[36,37]

The information encoded in the base-sequences of DNA provides a means to use oligonucleotides as a functional material for the assembly of microcapsules, and specifically, to construct stimuli-cleavable microcapsules. The base pairing of nucleic acids provides a general method to assemble microcapsules by interlinking DNA layers via hybridization.[38,39] Furthermore, by the appropriate design of the shell sequences, switchable, stimuli-responsive microcapsules undergoing signal-triggered degradation can be assembled.[40] Recently, the synthesis of DNA-based capsules, via the cross-linking of oligonucleotide layers by ATP aptamer bridges, was reported.[41] The ATP-triggered degradation of the microcapsules, by the removal of the bridging units, through the formation of the ATP-aptamer complexes and the accompanying release of loads encapsulated in the microcapsules, were reported.

The o-nitrobenzyl ester or phosphate ester derivatives are versatile photocleavable protective groups.[42,43] These photoprotective groups were widely implemented in organic synthesis,[44] uncaging of receptor units,[45] and photopatterning of surfaces.[46−49] In the present study, we report on the synthesis and characterization of photocleavable DNA-based microcapsules. We address the photochemically triggered degradation of the microcapsules and the release of a

Received: May 9, 2016
Published: June 16, 2016

DOI: 10.1021/jacs.6b04773
J. Am. Chem. Soc. 2016, 138, 8936−8945

macromolecular fluorescent load (tetramethylrhodamine-modified dextran, TMR-D) or of the catalytically active microperoxidase-11 oligopeptide, MP-11 load. We discuss the effect of the dose of irradiation and the number of photocleavable groups associated with the microcapsule shells on the efficiency of microcapsule degradation and the rates of load release. We further load the photocleavable microcapsules with the prodrug doxorubicin-modified dextran, DOX-D, and study its photoinduced release from the microcapsules. We further demonstrate the versatility of the preparation of all-DNA-stabilized microcapsules carrying payloads by the synthesis of pH-responsive microcapsules that release the loads at acidic pH values. We discuss the permeation features of the microcapsules into cancer cells, and address the photochemically triggered and pH-induced cytotoxicity of the microcapsules toward cancer cells.

■ RESULTS AND DISCUSSION

Figure 1 depicts the stepwise assembly of the photocleavable DNA capsules. Template $CaCO_3$ particles (~3.2 μm diameter) were loaded with TMR-D, MP-11, DOX-D, or CdSe/ZnS QDs using the coprecipitation method and following a reported procedure.[41] The particles were coated with a primary, positively charged, poly(allylaminehydrochloride), PAH (58 kDa) layer. The PAH-coated $CaCO_3$ particles acted then as a

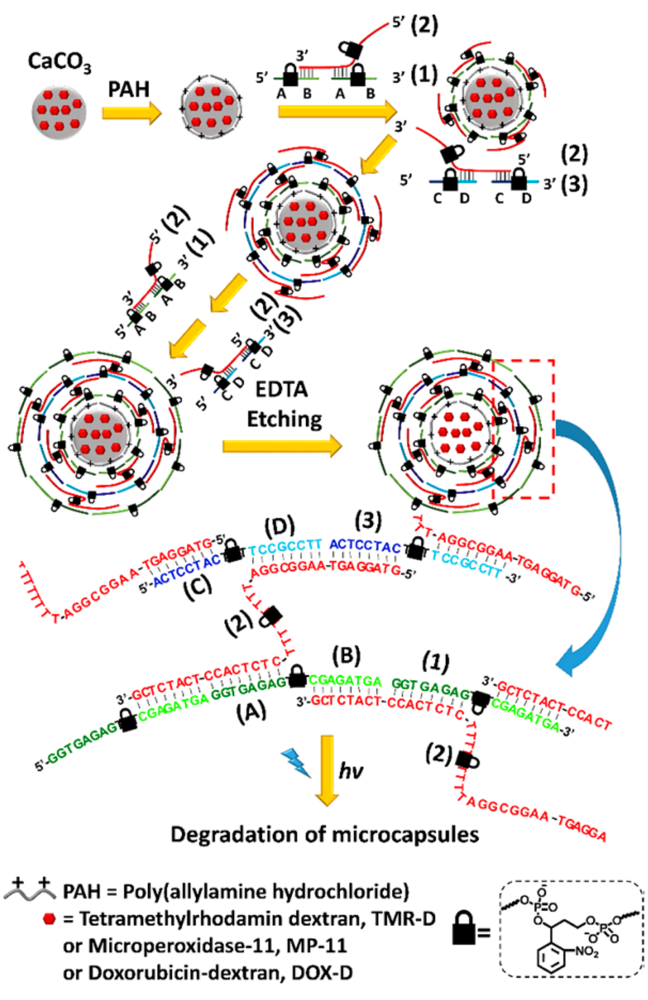

Figure 1. Schematic preparation of the photocleavable loaded microcapsules and the light-induced degradation of the microcapsules.

template for the deposition of six layers of the photocleavable DNA shell. The (**1**)/(**2**) hybrid composed of two units of DNA strand (**1**) hybridized with one unit of DNA strand (**2**) was electrostatically bound to the PAH-modified particles. It should be noted that the strand (**1**) includes two subdomains A and B that allow the hybridization of the two units of (**1**) with (**2**) via appropriate base complementarity and directionality of the subdomains with respect to the base-sequence of (**2**). Subsequently, the hybrid (**3**)/(**2**) was linked to the primary oligonucleotide layer. The strand (**3**) in the hybrid (**3**)/(**2**) includes two subdomains C and D that exhibit base complementarity and directionality that allows the formation of the hybrid (**3**)/(**2**) consisting of two units of (**3**) linked to one unit of (**2**). The linkage of the (**3**)/(**2**) layer to the primary oligonucleotide layer proceeds via the hybridization of the 5′-single-stranded tethers of (**2**) associated with the base layer with the free single-stranded tethers of subdomains C and D. By the sequential layer-by-layer deposition of the hybrid (**1**)/(**2**) and (**3**)/(**2**), a controlled number of oligonucleotide layers, bridged by the units (**2**), was assembled on the $CaCO_3$ microparticle template cores. Each subunit in the hybridized oligonucleotide layers (**1**)/(**2**) or (**3**)/(**2**) included an o-nitrobenzylphosphate photoactive group, and the bridging nucleic acid units (**2**) included, also, the o-nitrobenzylphosphate photoactive label (marked with a lock shape in Figure 1). The resulting photosensitive DNA-coated $CaCO_3$ particles were treated with EDTA to dissolve the core $CaCO_3$ to yield the TMR-D-, MP-11-, or DOX-D-loaded microcapsules. The loaded microcapsules were then irradiated with UV light (λ = 365 nm), and the photoinduced cleavage of the o-nitrobenzyl phosphate ester groups to the o-nitrosobenzophenone functionalities fragments the oligonucleotide shell of the microcapsules, resulting in the decomposition of the shell of the microcapsules, and the release of the respective loads (Movie S1). Note that the method to assemble the microcapsules allows us to control the number of oligonucleotide layers comprising the shell, and the density of the photocleavable labels on the different components (the density of the photocleavable units is anticipated to control the efficiency of degradation of the capsules and the rate of release of the loads).

In the first step we had to identify the desired number of photocleavable DNA layers that are implemented to stabilize the microcapsules to the extent that the photodegradation of the microcapsules, and the accompanying release of the loads, can be studied with minimal perturbations due to leakage of the loads across the shells. Toward this goal, a series of tetramethylrhodamine-modified dextran, TMR-D-loaded microcapsules, composed of different number of photocleavable cross-linked nucleic acid layers were prepared. Figure S1, type A of the microcapsules, included two layers of nucleic acids, each modified with the photocleavable label, where the two layers were interlinked by a photocleavable bridge. Type B of microcapsules included four layers of nucleic acid units, each modified with photocleavable units, where all bridging units were also modified with the photocleavable labels. Type C of microcapsules included six layers of nucleic acids modified with the photocleavable labels, and all bridging units were also functionalized with the photocleavable labels. The photosensitive microcapsules were irradiated with UV light (λ = 365 nm) for a fixed time-interval of 2 min, and the fluorescence intensity of TMR-D, released after a fixed time-interval of 1 h, was evaluated. For comparison, the fluorescence generated by the natural leakage of the load from the different classes of

DOI: 10.1021/jacs.6b04773
J. Am. Chem. Soc. 2016, 138, 8936−8945

nonilluminated microcapsules was examined. Figure S1 shows the experimental results. Evidently, a ca. 40%, 15%, and 7% leakage of the load, as compared to the photostimulated release of the load from the respective irradiated microcapsules, is observed for the two layer, four layer, and six layer shells, respectively. The minute leakage interference observed with the six layer-stabilized microcapsules dictated all further experiments that implemented photocleavable capsules composed of six stabilizing nucleic acid layers.

Figure 2A shows the SEM images of $CaCO_3$ particles prior to the modification with the DNA shells, panel I, after the deposition of the six-layer DNA shell, panel II, and after the dissolution of the $CaCO_3$ core with EDTA, panel III. The $CaCO_3$ particles (~3.2 μm diameter) show a smooth surface, and the DNA-coated template particles show a "hairy" surface, supporting the coating of the particles with DNA. After the dissolution of the core, the SEM images reveal a collapsed structure, while retaining the intact structure of the capsules. The collapsed state of the capsules is probably due to the vacuum conditions during the measurements (for other SEM images, see Figure S2). Figure 2B, panel I, depicts the fluorescence and bright-field microscopy images of the DNA-coated microcapsules prior to the dissolution of the core particles. The TMR-D-loaded particles show high fluorescence, and from overlapping the bright-field images (dark dots) capsule sizes of ca. 3.2 μm could be derived. Figure 2B, panel II, shows the fluorescence and bright-field microscopy images of the microcapsules after the EDTA-induced dissolution of the core. The bright-field images of the capsules reveal a brighter interior surrounded by a darker shell, consistent with the dissolution of the inorganic core. The dissolution of the core is accompanied by a shrinkage of the capsules to an average size of ca. 2.5 μm. From the number of cross-linked duplex DNA layers, we estimate the thickness of the shell to be ca. 35−40 nm. Flow cytometry experiments indicated that the preparation protocol generated a suspension of 10100 TMR-D-loaded microcapsules/μL solution. The confocal microscopy images reveal that the DNA-protected microcapsules do not aggregate and exist as single particles, and represent a major advantage of DNA-based microcapsules. This phenomenon is attributed to electrostatic repulsive interactions between the DNA shells of the microcapsules.

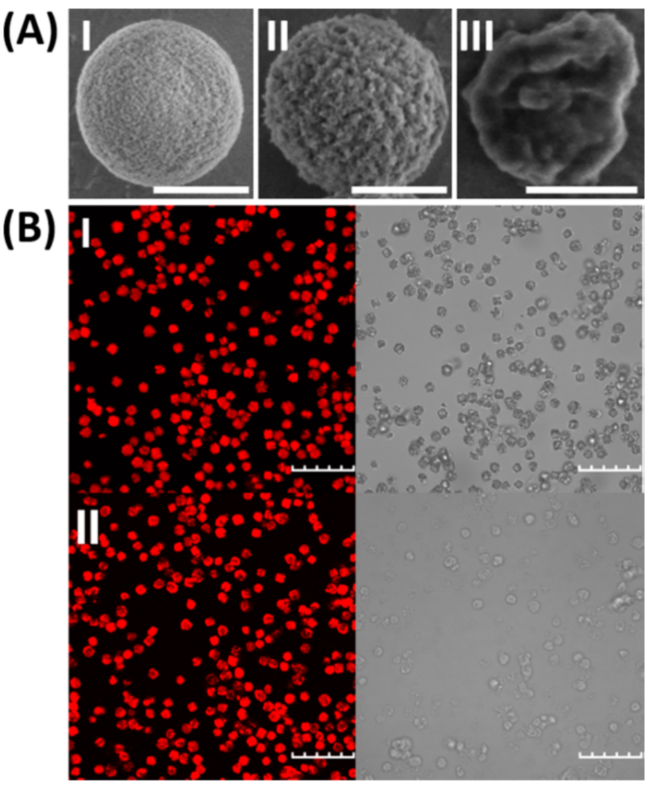

Figure 2. (A) SEM images corresponding to (I) uncoated $CaCO_3$ particles, (II) DNA-coated $CaCO_3$ particles, and (III) microcapsules treated with EDTA to dissolve the core (scale bar: 2 μm, see Supporting Information for additional images). (B) Confocal fluorescence and bright-field microscopy images of (I) DNA-coated $CaCO_3$ particles and (II) treatment with EDTA. Microcapsules were loaded with TMR-D. Scale bar is 20 μm.

The schematic photochemical unlocking of the capsules and the triggered release of TMR-D, as a result of the photodegradation of the microcapsules, are depicted in Figure 3A.

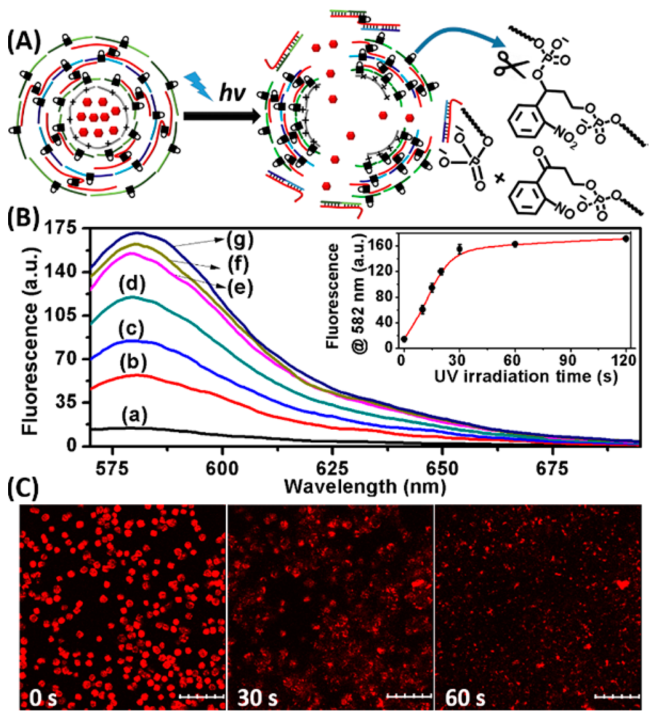

Figure 3. (A) Schematic light-induced release of TMR-D from the photocleavable microcapsules. (B) Fluorescence spectra of the released TMR-D load observed upon the irradiation of the TMR-D-loaded microcapsules for different time-intervals corresponding to (a) 0 s, (b) 10 s, (c) 15 s, (d) 20 s, (e) 30 s, (f) 1 min, and (g) 2 min, and allowing the release of the load for a fixed time-interval of 30 min. Inset: Derived calibration curve of the fluorescence generated by the TMR-D that is released upon the irradiation of the microcapsules for different time-intervals. In all experiments the irradiated volume correspond to 40 μL, 500 microcapsules/μL. (C) Confocal images corresponding to the TMR-D-loaded microcapsules upon irradiation for different time-intervals. Scale bar is 20 μm.

The photoirradiation of the capsules (λ = 365 nm) resulted in the cleavage of the o-nitrobenzyl linkers that formed o-nitrosobenzophenone units, leading to the decomposition of the microcapsules and the release of the TMR-D fluorescent load. Figure 3B shows the fluorescence intensities of the released dyes after a fixed time-interval of 30 min, upon irradiation of microcapsule samples of identical content, for

DOI: 10.1021/jacs.6b04773
J. Am. Chem. Soc. 2016, 138, 8936−8945

different time-intervals with a light source, λ = 365 nm, P = 35 mW/cm^2. While nonirradiated microcapsules resulted in a negligible amount of released TMR-D, the fluorescence intensities of the released fluorescent loads were higher as the time-intervals of irradiation were prolonged, and after ca. 40 s of irradiation the fluorescence intensity reached a saturation value, implying that all microcapsules were degraded after this time-interval. Using an appropriate calibration curve of TMR-D fluorescence versus concentration (Figure S3A), we estimate the released load concentration to be ca. 64 nM TMR-D. Figure 3C shows the fluorescence images of the TMR-D-loaded microcapsules upon irradiation for 30 and 60 s. After 30 s most of the microcapsules degraded, and after 60 s complete degradation of the microcapsules is evident.

The photochemically induced release of microperoxidase-11, MP-11, from the MP-11-loaded microcapsules was similarly examined. The MP-11 is a heme-containing peptide that mimics the catalytic functions of cytochrome c. Specifically, MP-11 catalyzes the H_2O_2-mediated oxidation of Amplex UltraRed to the fluorescent product Resorufin, Figure 4A. The

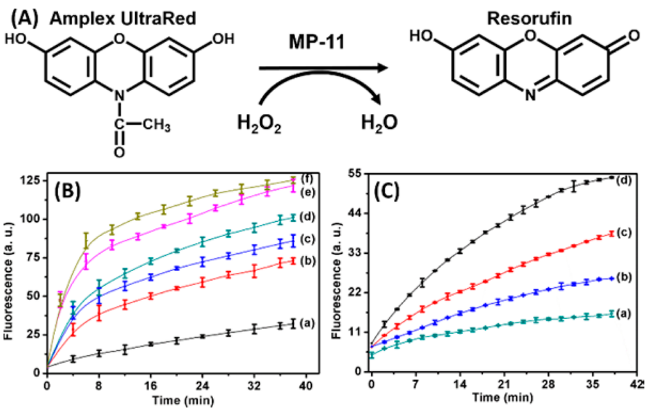

Figure 4. (A) MP-11-catalyzed oxidation of Amplex UltraRed to Resorufin by H_2O_2. (B) Probing the photochemically triggered release of MP-11 from the photosensitive microcapsules via the secondary time-dependent MP-11-catalyzed oxidation of Amplex UltraRed to resorufin by H_2O_2. The MP-11-loaded microcapsules were irradiated, λ = 365 nm, for different time-intervals: (a) 0 s, (b) 10 s, (c) 15 s, (d) 20 s, (e) 1 min, and (f) 2 min. The release of MP-11 from the irradiated microcapsules was allowed to proceed for 2 h, and subsequently, the microcapsules were precipitated and removed from the samples. The content of the released MP-11 was then followed by probing the catalyzed oxidation of Amplex UltraRed to Resorufin by H_2O_2. (C) Probing the time-dependent release of MP-11 from the irradiated, λ = 365 nm, microcapsules by assaying the activity of the released MP-11 by the catalyzed oxidation of Amplex UltraRed to Resorufin by H_2O_2. Samples were irradiated for a fixed time-interval of 20 s, and the release of MP-11 was allowed to proceed for different time-intervals: (a) 30 min, (b) 50 min, (c) 70 min, and (d) 120 min. Subsequently, the microcapsules were separated, and the content of the released MP-11 was assayed by the MP-11-catalyzed oxidation of Amplex UltraRed to the fluorescent Resorufin.

effect of the light-induced unlocking of the MP-11-loaded microcapsules (six oligonucleotide layers) on the release of MP-11 from the capsules is displayed in Figure 4B. In these experiments, the microcapsules are illuminated for different time-intervals (λ = 365 nm), and the MP-11 loads are released from the capsules for a fixed time-interval of 120 min. Subsequently, the microcapsules were precipitated and separated, and the activities of the released MP-11 were monitored via the H_2O_2-mediated oxidation of the Amplex UltraRed to the fluorescent product Resorufin. Evidently, as the time-interval of irradiation increases, the biocatalyzed oxidation of Amplex UltraRed is enhanced, consistent with the higher degree of photochemical degradation of the microcapsules. After 2 min of irradiation the rate of Amplex UltraRed oxidation reaches a saturation value, implying that, after this time-interval of illumination, all of the loaded MP-11 was released from the microcapsules within the time-interval of 120 min. Figure 4C depicts the time-dependent fluorescence changes by the MP-11-catalyzed oxidation of Amplex UltraRed upon irradiation of the six-layer-stabilized microcapsules for 20 s and allowing the release of the MP-11 from the photo-irradiated microcapsules for different time-intervals. As the time-interval of the release of MP-11 is prolonged, the biocatalyzed oxidation of Amplex UltraRed by H_2O_2 is enhanced, consistent with the increased content of released MP-11. Using an appropriate calibration curve (Figure S3 B), we estimate that the content of MP-11 released after 120 min corresponded to ca. 14 μg/mL. Note that the release of MP-11 is slower than the release of TMR-D from the capsules. Presumably, electrostatic interactions between the peptide and the nucleic acids and/or $\pi-\pi$ interactions between the hemin units associated with MP-11 with the oligonucleotide units retard the release of the load. As a result, a higher degree of photochemical fragmentation of the shell is required to release the MP-11.

We further examined the effect of loading of the shell composition with the photodegradable labels on the efficiency of photodegradation of the microcapsules, and the release of the loads. These experiments used six-layer-stabilized micro-capsules that included TMR-D, as load. The microcapsules were constructed, however, to include a programmed number of DNA shells that are modified or nonmodified with the photosensitive o-nitrobenzyl phosphate ester groups. Figure 5 depicts schematically the microcapsule constructs that were investigated: In construct I, the first, third, and fifth DNA layers are labeled with the photocleavable labels, while the second, fourth, and sixth layers are nonlabeled. The one/two, two/three, three/four, four/five, and five/six layers are bridged by nucleic acids carrying the photocleavable groups. In construct

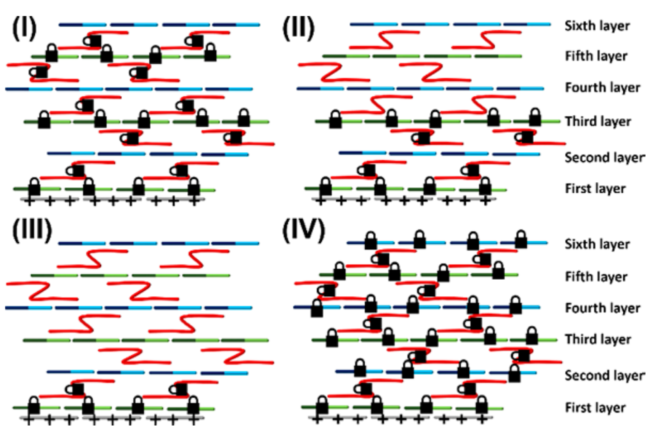

Figure 5. Schematic structures of the DNA microcapsules that include different numbers of photocleavable layers. (I) First, third, and fifth layers include the photocleavable units. (II) First and third layers include the photocleavable units. (III) Only the first layer includes the photocleavable units. (IV) All six layers include the photocleavable units.

DOI: 10.1021/jacs.6b04773
J. Am. Chem. Soc. 2016, 138, 8936−8945

II, the DNA layers one and three are labeled with the photodegradable labels, while the nucleic acid layers two, four, five, and six are unlabeled. The layers one/two and two/three layers are interlinked by the nucleic acid bridge carrying the photocleavable bridging units. In construct III only the first layer is labeled with the photocleavable label, while nucleic acid layers two, three, four, five, and six are nonlabeled. The first layer is linked, however, to the second nonlabeled nucleic acid layer by a bridging unit carrying the photocleavable label. The fully labeled six layer shell is depicted, for comparison, in construct IV.

Figure 6 depicts the time-dependent release of the fluorescent label, TMR-D, from the different microcapsule constructs, while comparing the results to the release of the fluorescent loads from the six layer-stabilized microcapsules modified in all layers and all bridging units, construct IV. In these experiments, the different microcapsules were irradiated for a fixed time-interval of 2 min, followed by the characterization of the time-dependent release of the fluorescent loads from the degraded microcapsules. The release of the fluorescent load from the all-six layer labeled nucleic-acid-stabilized microcapsules is complete within a time-interval of 12 min (curve a). In turn, the irradiation of the microcapsules exhibiting construct I leads to a substantially slower release of load, and the release is incomplete even after a time-interval of 120 min (curve b). In turn, the irradiation of the microcapsules composed of constructs II and III did not show significant release of the fluorescent load, even after a time-interval of 120 min (curves c and d). These results clearly indicate that the density of the photocleavable labels strongly affects the efficiency of release of the load from the capsules (further support demonstrating the relation between the degree of modification of the microcapsules shells with the photocleavable groups and the efficiency of release of the load was obtained by time-dependent confocal microscopy imaging of the microcapsules exhibiting constructs I and II, see Figures S3 and S4). It should be noted that although a six-layer coating shell protects oligmers (MW ≥ 1800), polymer loads, or nanoparticles from diffusion across the DNA shell, lower molecular weight loads (MW ≤ 500), e.g., fluorescein, Texas-Red, reveal permeability through the shell without unlocking of the shell. This is the reason that the doxorubicin was loaded on the dextran load, DOX-D, to inhibit uncontrolled diffusion from the microcapsules (for detailed discussion vide infra).

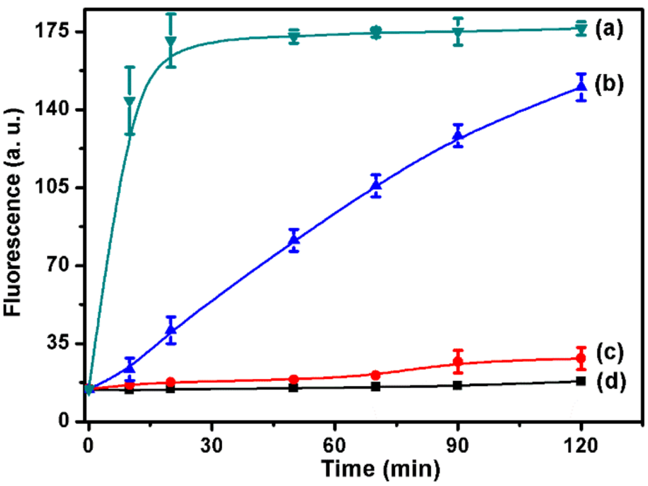

Figure 6. Time-dependent release of TMR-D from the capsules with different numbers of photocleavable layers, upon 2 min of irradiation, λ = 365 nm. The compositions of the shells of the capsules are detailed in Figure 5: (a) configuration IV, (b) configuration I, (c) configuration II, and (d) configuration III.

The light-responsive microcapsules were further implemented to demonstrate the light-triggered release of a drug, e.g., the anticancer drug doxorubicin, DOX, linked to dextran DOX-D, Figure 7A. Toward this goal, the doxorubicin-drug was covalently linked to dextran via boronic ester bonds. The covalent linkage of DOX to dextran is needed to eliminate the uncontrolled diffusional release of the low-molecular-weight DOX from the microcapsules. The specific boronate ester linkage between DOX and the dextran was selected since the boronic ester bond is cleavable at acidic pH values (pH ≤ 6) present in cancer cells (vide infra, cell experiments). Thus, the photochemically released DOX-D may be considered as a prodrug, where the secondary hydrolytic uncaging of doxorubicin from the dextran backbone yields the drug. We note, however, that DOX-D exhibits very low fluorescence, in contrast to the high fluorescence intensity of DOX itself. Accordingly, in all in vitro release experiments of DOX-D from the microcapsules, the solution of DOX-D was acidified to yield free DOX. Microcapsules consisting of six DNA layers composed of (**1**) and (**3**) cross-linked by (**2**) were loaded with DOX-D, cf.

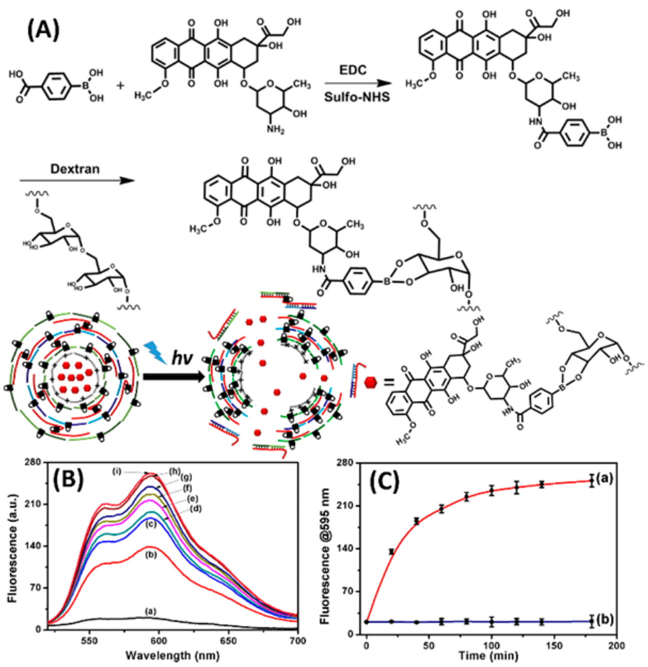

Figure 7. (A) Synthesis of the doxorubicin-modified dextran, DOX-D, and the schematic phototriggered release of DOX-D from the microcapsules. (B) Fluorescence spectra corresponding to the released doxorubicin upon irradiation of the photocleavable microcapsules for different time-intervals: (a) 0 s, (b) 10 s, (c) 15 s, (d) 20 s, (e) 30 s, (f) 1 min, (g) 2 min, (h) 3 min, and (i) 5 min. The release of DOX-D from the irradiated samples was allowed to proceed for 1 h, and subsequently, the microcapsules were precipitated and separated. The solution containing the released DOX-D was acidified to pH = 6.0 to allow the cleavage of the fluorescent DOX from the dextran carrier. (C) Time-dependent release of DOX-D from (a) the irradiated DOX-D-loaded microcapsules irradiated for 20 s; (b) nonirradiated DOX-D-loaded microcapsules. The content of the released DOX-D from the respective samples was evaluated as described in part B.

DOI: 10.1021/jacs.6b04773
J. Am. Chem. Soc. 2016, 138, 8936−8945

Figure 1. (All layers and bridging units included the photocleavable units.)

Figure 7B depicts the fluorescence spectra of the released DOX-D upon irradiation of the capsules for a variable time-interval and following the content of DOX-D after a fixed time-interval of 1 h. As the time of irradiation is prolonged, the content of released DOX-D increases, consistent with the higher degree of degradation of the microcapsules, at longer time-intervals of irradiation. We note that the microcapsules irradiated for 3 or 5 min release similar contents of DOX-D after a time-interval of 1 h. Furthermore, the fluorescence spectra of the released DOX-D do not change upon further prolongation of the release process. These results suggest that the fluorescence spectra observed in Figure 7B, curves h and i, correspond to the unlocking of all microcapsules, resulting in the release of all the loads. Using an appropriate calibration curve of DOX-D (Figure S3D), we estimate that an average load release of ca. 46 nM DOX-D occurred. Figure 7C depicts the time-dependent fluorescence of DOX-D from the micro-capsules irradiated for a time-interval of 20 s. Evidently, the amount of released DOX-D increases with time, and it levels off to a saturation value after ca. 80 min. The saturated fluorescence intensity corresponds to the complete release of DOX-D from the photochemically unlocked microcapsules.

In the next step we have performed preliminary experiments examining the penetration of the photoresponsive micro-capsules into cells, and the cytotoxicity of the DOX-dextran-loaded microcapsules toward the cells. Accordingly, we have loaded the photocleavable microcapsules with CdSe/ZnS QDs (λ_{em} = 560 nm), as luminescent labels. Malignant MDA-MB-231 breast cancer cells and MCF-10A normal epithelial breast cells were treated with the luminescent microcapsules. Figure 8A, panels I–III and panels IV–VI, depicts the phase images, the fluorescence microscopy images, and the merged images of the MCF-10A and the MDA-MB-231 cells. The fluorescence images indicate that the CdSe/ZnS-loaded microcapsules penetrate effectively into the MDA-MB-231 cancer cells, while almost no penetration of the microcapsules into the normal breast epithelial cells is observed. Figure 8B shows the preliminary cytotoxicity studies examined upon treating the MCF-10A or the MDA-MB-231 cells with the DOX-dextran-loaded microcapsules upon illumination, panel I, and without illumination, panel II. The irradiated samples of the MCF-10A (blue bars) and MDA-MB-231 (red bars) cells (irradiation time 5 min) revealed, after a time-interval of 24 h, a cell death corresponding to ca. 5% and 25%, respectively. Control experiments, where the cells were irradiated with DOX-dextran-unloaded microcapsules revealed a very low cell death of the MCF-10A and MDA-MB-231 cells (4–5%). Figure 8B, panel II, shows the results corresponding to the cell viability of the nonirradiated MCF-10A and MDA-MB-231 cells subjected to the DOX-dextran-loaded microcapsules. Evidently, both types of cells subjected to nonirradiated microcapsules reveal minute cell death (6–7%). The results demonstrate selective cytotoxicity toward the cancer cells upon irradiation of the DOX-dextran-loaded microcapsules. These results are consistent with the preferred penetration of the DOX-dextran-loaded microcapsules into the MDA-MB-231 cancer cells and with the light-stimulated cytotoxicity of the microcapsules that involves the intracellular photocleavage of the microcapsules and the release of the drug. Nonetheless, it should be noted that the resulting cytotoxicity is quite limited, and further optimization of the system by improving the permeability of the micro-capsules into the cancer cells, the application of higher doses of irradiation, and eventually, the substitution of the photo-cleavable groups by light-sensitive units operating in the visible region are essential parameters to address. Although the mechanism for the preferred penetration of the DOX-D-loaded microcapsules into the MDA-MB-231 cells is, at present, unknown, the improved penetration of microcapsules might be attributed to the enhanced permeability and retention (EPR) effect where enhanced delivery of nanoparticles or liposomes into cancer cells was observed.[50]

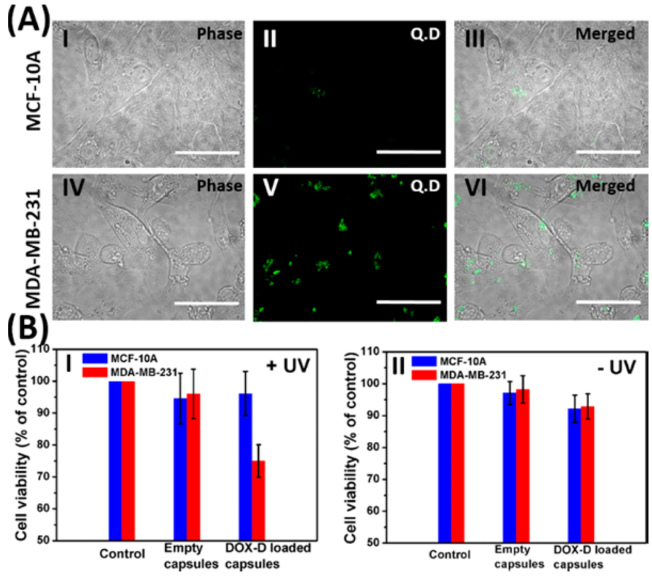

Figure 8. (A) Microscopy images corresponding to the uptake of photocleavable microcapsules loaded with CdSe/ZnS QDs by MCF-10A (normal breast cells) and MDA-MB-231 (breast cancer cells). Scale bar is 100 μm. (B) Cytotoxicity of empty capsules and DOX-D-loaded microcapsules toward normal (MCF-10A, blue) and malignant (MDA-MB-231, red) breast epithelial cells (error bars derived from n = 3 experiments). Panel I: Upon irradiation of the cells for 5 min and assaying the viability of the cells after 24 h. Panel II: Viability of nonirradiated cells incubated with the photocleavable empty or DOX-D-loaded microcapsules after 24 h.

Furthermore, in order to show the generality of fabrication of stimuli-responsive all-DNA microcapsules, we decided to implement the paradigm for the preparation of pH-responsive microcapsules that are unlocked upon treatment at acidic pH (pH = 5.0) as a result of the reconfiguration of the interlayer DNA bridging units into an i-motif structure. Figure 9A outlines the preparation of pH-responsive CdSe/ZnS QDs-loaded microcapsules. The PAH-coated CdSe/ZnS QDs-loaded $CaCO_3$ microcapsules were subjected to a layer-by-layer deposition process of the layer (**4**)/(**5**)/(**8**)/(**6**)/(**7**) cross-linked to the layer composed of (**4**)/(**5**)/(**10**)/(**6**)/(**7**) by the bridging unit (**9**). The $CaCO_3$ microcapsules were coated with 6 layers of the DNA constituents. After dissolution of the $CaCO_3$ core units, the CdSe/ZnS-loaded microcapsules were formed. For the confocal microscopy images and the SEM images of the microcapsules, see Figure 10. The sequences (**4**), (**5**), (**6**), and (**7**), marked red, are rich in cytosine bases capable of forming the i-motif structure at pH = 5.0.

The principle to unlock the microcapsules is depicted in Figure 9B. At pH = 5.0 the cytosine-rich sequences reconfigure into the i-motif structure that results in the decomposition of the microcapsules. Figure 11A depicts the fluorescence spectra

DOI: 10.1021/jacs.6b04773
J. Am. Chem. Soc. 2016, 138, 8936–8945

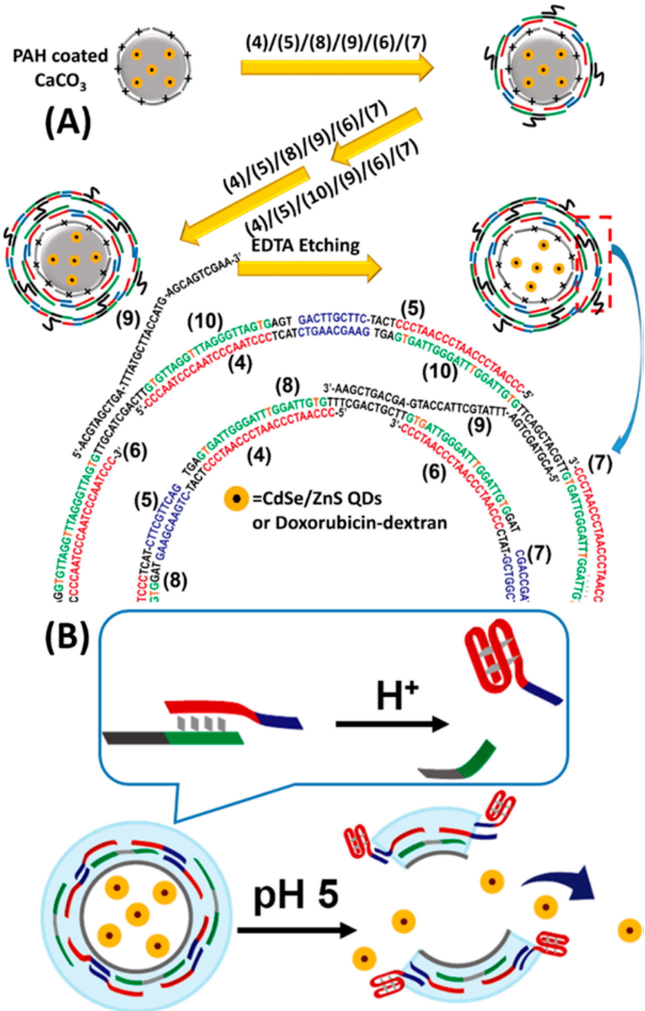

Figure 9. (A) Schematic illustration of the preparation of pH-responsive DNA microcapsules loaded with CdSe/ZnS QDs or the anticancer drug, DOX-D. (B) Principle of pH-induced microcapsules unlocking and loads releasing via the formation of i-motif structure at pH = 5.0.

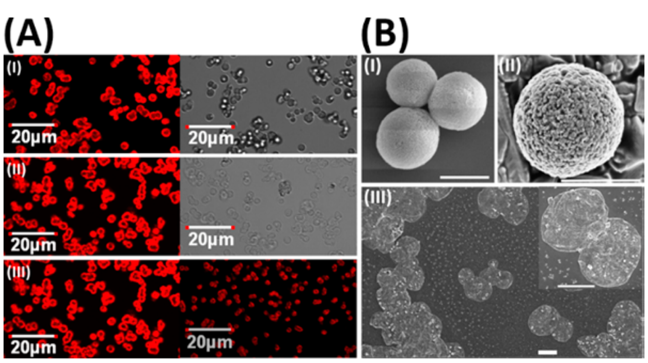

Figure 10. (A) Confocal fluorescence and bright-field microscopy images of (I) DNA-coated $CaCO_3$ particles, (II) treatment with EDTA, and (III) DNA microcapsules without (left side) and with addition of acid (right side). Microcapsules were loaded with CdSe/ZnS QDs (λ_{em} = 620 nm). (B) SEM images corresponding to (I) uncoated $CaCO_3$ particles, (II) DNA-coated $CaCO_3$ particles, and (III) microcapsules treated with EDTA to dissolve the core, scale bar: 2 μm.

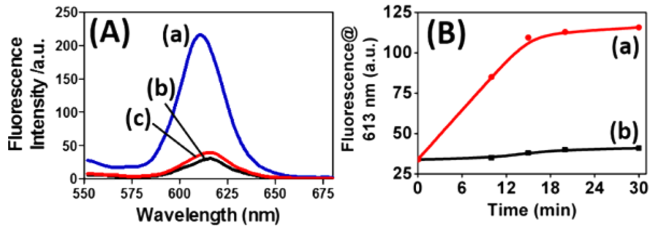

Figure 11. (A) Fluorescence spectra corresponding to the release of CdSe/ZnS QDs upon treatment of the pH-responsive microcapsules at different pH, for a fixed time-interval of 30 min: (a) pH = 5.0, (b) pH = 7.0, and (c) pH = 9.0. (B) Time-dependent release of CdSe/ZnS QDs upon treatment of the microcapsules at (a) pH = 5.0 and (b) pH = 7.0.

corresponding to the released CdSe/ZnS QDs from the microcapsules after a time-interval of 30 min at pH = 5.0 (a), pH = 7.0 (b), and pH = 9.0 (c). Evidently, the QDs are effectively released from the microcapsules at pH = 5.0, while only minute leakage of the QDs is observed at pH = 7.0 or pH = 9.0. Figure 11B depicts the fluorescence changes upon the time-dependent release of the QDs at pH = 5.0, and pH = 7.0. Evidently, the release is selective and proceeds effectively only upon the dissociation of the microcapsules at pH = 5.0, due to the reconfiguration of the layers constituting the shells into i-motif structures. A major issue related to the implementation of all-DNA microcapsules, as stimuli-responsive carriers, rests on the scalability of the synthesis of the loaded microcapsules. To support the scalability of the synthetic procedure, we examined the possibility to increase by a factor of 6-fold the content of the resulting loaded microcapsules. In the experiment shown in Figure 10, we used 1 mg of $CaCO_3$ to produce a buffer solution of 50 μL that included 10240 microcapsules/μL. By increasing the content of $CaCO_3$ to 6 mg and increasing 6-fold the volume of the DNA constituents, we yielded a final volume of 300 μL that included 11040 microcapsules/μL. We find that, after preparation of the loaded microcapsules, and their precipitation, ca. 70% of the DNA used to assemble the microcapsules is present in the solutions synthesizing the microcapsules. By readjusting the concentrations of the layer constituents of DNA solutions, the subsequent addition of PAH-modified $CaCO_3$ particles allowed the second-phase preparation of the pH-responsive microcapsules at a concentration of ca. 11000 microcapsules/μL. These results suggest that the processing of the microcapsules can be scaled without affecting the quality of the microcapsules.

Preliminary intracellular experiments probed the effect of the DOX-D-loaded pH-responsive microcapsules on MDA-MB-231 breast cancer cells and MCF-10A epithelial breast cells, Figure S6. We find that after a time-interval of 5 days, ca. 25% cell death was observed for the MDA-MB-231 cells, and no cytotoxic effect was detected on the MCF-10A cells. Presumably, the acidic pH environment in the cancer cells induced the unlocking of the capsules, and the uncaging of free DOX from the dextran polymer by the acid-catalyzed hydrolysis of the boronate ester group led to the formation of the free drug.

■ CONCLUSIONS

The present study has introduced the synthesis of light- and pH-responsive DNA-based microcapsules for the release of loads incorporated in the microcapsule carriers. The light-responsive microcapsules are based on the assembly of o-

DOI: 10.1021/jacs.6b04773
J. Am. Chem. Soc. 2016, 138, 8936−8945

nitrobenzyl photocleavable groups associated with the DNA layer stabilizing the shells of the microcapsules. Upon photocleavage of the o-nitrobenzyl groups, the microcapsules were degraded leading to the release of the loads. Specifically, we demonstrated the light-induced release of TMR-D or MP-11 from the microcapsules, as drug models. The study has, also, addressed the effect of the number of photocleavable units associated with the layered DNA shells on the effectiveness of the photoinduced release of the loads. We have further implemented the photocleavable DNA microcapsules as carriers for the light-induced release of the anticancer drug doxorubicin. Preliminary experiments probed the permeation of the photocleavable microcapsules into cells, and the cytotoxicity of the DOX-D-loaded microcapsules on the cells. Encouraging results demonstrating the cytotoxicity of the DOX-D-loaded microcapsules toward cancer cells were observed. Selective permeation of DOX-D-loaded microcapsules into MDA-MB-231 breast cancer cells was demonstrated, and the superior cytotoxicity of the DOX-D-loaded microcapsules toward cancer cells, as compared to normal cells, was achieved. The use of UV light (λ = 365 nm) for the photodegradation of the microcapsules and the release of the drugs is certainly a disadvantage. The lack of UV light penetration into tissues, and the harmful effect of UV light on cells, would be a drawback for the practical applications of the photocleavable groups as drug carrier. We wish to emphasize, however, that the present photocleavable, light-responsive microcapsules as drug carriers should be considered only as a model paradigm. The present commercial availability of o-nitrosobenzyl-functionalized nucleotides enabled us to materialize and develop the concept. The availability of photocleavable protecting groups undergoing photocleavage in the visible and IR regions (using two-photon IR excitation) is well-documented.[51] The future implementation of such photoresponsive cleavable groups seems feasible. Also, the use of optical fibers guiding the UV light to target tissues might be a method to unlock the drug-loaded o-nitrobenzyl-photocleavable microcapsules at specific organs with minimal harm. Furthermore, one might use the photocleavable drug-loaded microcapsules for the treatment of melanoma cancer or other skin diseases (e.g., Leishmania) that do not require deep UV light penetration.

The diversity of the synthetic methodology to assemble stimuli-responsive DNA-based microcapsules was further demonstrated by the construction of pH-responsive microcapsules loaded with QDs (as drug model) or with the caged DOX-D pro-drug. Specifically, we constructed DNA-stabilized microcapsules consisting of nucleic acids that are reconfigured at acidic pH values to i-motif structures, thereby dissociating the shells and releasing the loads. The development of pH-responsive microcapsules is promising since the acidic conditions in cancer cells could provide a mechanism for the specific unlocking and release of the anticancer drug in these cells. Indeed, the preliminary experiments support this concept, and specific cytotoxicity toward cancer cells was demonstrated. Nonetheless, the optimization of the systems seems to be an important future goal.

■ EXPERIMENTAL SECTION

Reagents and Materials. Magnesium chloride, sodium chloride, 4-(2-hydroxyethyl)-piperazine-1-ethanesulfonic acid (HEPES acid), 4-(2-hydroxyethyl)-piperazine-1-ethanesulfonic acid sodium salt (HEPES base), poly(allylamine hydrochloride) (PAH, 58 kDa MW), ethylenediaminetetraacetic acid disodium salt dihydrate (EDTA), microperoxidase-11 (MP-11), and hydrogen peroxide (H_2O_2) were purchased from Sigma-Aldrich. Amplex UltraRed Reagent and tetramethylrhodamine-dextran (TMR-D, 70 kDa MW) were purchased from Life Technologies Corporation. Doxorubicin hydrochloride, dextran (40 kDa MW), *N*-(3-(dimethylamino)propyl)-*N*′-ethylcarbodiimide hydrochloride (EDC), 4-carboxyphenylboronic acid, and *N*-hydroxysulfosuccinimide sodium salt (Sulfo-NHS) were purchased from Sigma-Aldrich. All oligonucleotides were synthesized and HPLC purified by Integrated DNA Technologies, Inc., and supplied in desalting form. Ultrapure water from a NANO pure Diamond (Barnstead Int., Dubuque, IA) source was used in all experiments. The sequences of the different strands used in the study (PC represents a photocleavable linker) are (**1**) 5′-GGTGAGAGT//PC//TCGAGATGA-3′, (**2**) 5′-GTAGGAGTAAGGCGGATTTT//PC//TTTTCTCTCACCTCATCTCG-3′, (**3**) 5′-ACTCCTACT//PC//TTCCGCCTT-3′, (**1a**) 5′-GGTGAGAGTTTCGAGATGA-3′, (**2a**) 5′-GTAGGAGTAAGGCGGATTTTTTTTTTCT-CTCACCTCATCTCG-3′, (**3a**) 5′-ACTCCTACTTTTCCGCCTT-3′, (**4**) 5′-CCCAATCCCAATCCCAATCCCTCATCTGAACGAAG-3′, (**5**) 5′-CCCAATCCCAATCCCAATCCCTCATCTTCGTTCAG-3′, (**6**) 5′-ATATCGGTCGTATCCCCAATCCCAATCCCAATCCC-3′, (**7**) 5′-CGACCGATATTATCCCCAATCCCAATCCCAATCCC-3′, (**8**) 5′-TGAGTGATTGGGATTTGGATTGTG-TTTCGACTGCTTGTGATTGGGATTTGGATTGTGGAT-3′, (**9**) 5′-ACGTAGCTGATTTATGCTTACCATGAGCAGTCGAA-3′, (**10**) 5′-TGAGTGATTGGGATTTGGATTGTGTTCAGCTAC-GTTGTGATTGGGATTTGGATTGTGGAT-3′.

Synthesis of Doxorubicin Conjugated to Dextran. Doxorubicin was premodified with 4-carboxyphenylboronic acid, followed by linking the doxorubicin boronic acid to dextran to yield the respective boronic ester. EDC (0.8 mg) and sulfo-NHS (2.2 mg) were added to 1.4 mL of 0.5 mM 4-carboxyphenylboronic acid solution (in 10 mM HEPES buffer solution, pH 7, containing 500 mM NaCl), and the mixture was allowed to react for 15 min at room temperature. A 100 μL portion of 10 mM doxorubicin was added to the mixture that was allowed to react at room temperature for 2 h with shaking followed by incubation at 4 °C overnight. A 2 mL portion of dextran solution (0.089 mg/mL in 10 mM HEPES, pH 10) was added to the mixture that was further allowed to react at room temperature for 2 h, with shaking followed by incubation overnight at 4 °C. The product was purified and separated from free doxorubicin using a centrifugal filter devices (Amicon, 10K MWCO) to yield after centrifugation 100 μL of the doxorubicin-dextran conjugate (44 μM). Using the appropriate calibration curve of free DOX (Figure S3C) and knowing the concentration of DOX-D, we estimate an average loading of 60 doxorubicin units on one dextran chain.

Preparation of $CaCO_3$ Microparticles with Different Loads. $CaCO_3$ particles were prepared by a precipitation reaction between equal amounts of $CaCl_2$ and Na_2CO_3 under magnetic stirring at room temperature, as described previously. The $CaCO_3$ particles were loaded by coprecipitation of the $CaCO_3$ particles in the presence of tetramethylrhodamine-modified dextran, TMR-D, by mixing of $CaCl_2$ (300 μL, 0.33 M) and Na_2CO_3 (300 μL, 0.33 M) solution, in the presence of TMR-D (30 μL, 6.25 mg/mL). Deionized water was added to obtain a total volume of 1020 μL. After magnetic stirring for 110 s, the suspension was left for 50 s at room temperature to settle down. The particles were centrifuged at 900 rpm for 20 s, followed by the removal of the supernatant solution. The resulting particles were washed by their resuspension and precipitation three times using 300 μL buffer, to remove byproducts resulting from the precipitation reaction. Microperoxidase-11, DOX-D, and CdSe/ZnS QDs-loaded capsules were prepared by a similar method, using the coprecipitation procedure. The final concentrations of MP-11, DOX-D, and CdSe/ZnS QDs-loads associated with the microcapsules corresponded to 2 mg/mL, 0.3 mg/mL, and 0.8 μM respectively.

Synthesis of Layer-by-Layer (LbL) DNA-Assembled Microcapsules. $CaCO_3$ microparticles (6 mg) were suspended in 1 mg/mL PAH solution (in 10 mM HEPES, pH 7, containing 500 mM NaCl) under continuous shaking. After an incubation time-interval of 20 min, the particles were precipitated and washed twice with 10 mM HEPES

DOI: 10.1021/jacs.6b04773
J. Am. Chem. Soc. 2016, 138, 8936−8945

buffer (pH 7, containing 500 mM NaCl) followed by centrifuging at 900 rpm for 20 s. The resulting PAH-modified $CaCO_3$ microparticles were coated by sequential incubation of the particles in the DNA hybrid (**1**)/(**2**) or (**3**)/(**2**) solutions for 30 min [5 μM in 10 mM HEPES, pH 7, containing 500 mM NaCl and 50 mM $MgCl_2$, the ratio of (**1**) to (**2**) and (**3**) to (**2**) was 2 to 1]. After each adsorption step, microparticles were washed using HEPES buffer (10 mM HEPES, pH 7, containing 500 mM NaCl) to remove nonadsorbed nucleic acids. Six layers of nucleic acids were deposited in total. Nucleic acids without photocleavable linker [(**1a**), (**2a**), and (**3a**)] were used to control the number of photodegradable layers in fabricated microparticles. pH-responsive DNA microcapsules were prepared by coating the PAH-modified $CaCO_3$ particles with i-motif sequence embedded DNA hybrids. The particles, loaded with CdSe/ZnS QDs or DOX-D, were sequentially incubated in 300 μL of (**4**), 5 μM/(**5**), 5 μM/(**8**), 10 μM/(**9**), 5 μM/(**6**), 5 μM/(**7**), 5 μM, solution or (**4**), 5 μM/(**5**), 5 μM/(**10**), 10 μM/(**9**), 5 μM/(**6**), 5 μM/(**7**), 5 μM, solution, consisted of 10 mM HEPES, pH 7, 500 mM NaCl, and 50 mM $MgCl_2$, for 30 min. After each adsorption step, particles were washed by HEPES buffer (10 mM HEPES, pH 7, containing 500 mM NaCl) to remove nonadsorbed nucleic acids. A total of six layers of DNA were deposited for the synthesis of i-motif sequence assembled microparticles. After the layer-by-layer assembly of the DNA shells, the template cores were dissolved by adding 0.1 M EDTA under gentle rotation. After the suspension became clear, the supernatant EDTA solution was removed by slow centrifugation to avoid aggregation of the DNA capsules. The capsules were washed three times with 10 mM HEPES buffer (pH 7, containing 500 mM NaCl) followed by centrifugation at 500 rpm for 20 min.

Characterization of Microparticles. Bright-field microscopy and fluorescence microscopy images of $CaCO_3$ particles and DNA capsules were taken using a FV-1000 confocal microscope (Olympus, Japan) equipped with an IX81 inverted microscope. A 60× /1.3 oil immersion objective was used. SEM images were recorded with a Magellan XHR 400L SEM operated at an acceleration voltage of 3 kV. An iCyt Eclipse Analyzer Flow Cytometer was used to count the number of capsules.

UV Irradiation-Induced Unlocking of the Microcapsules and the Release of the Entrapped Loads. The capsule solutions, 40 μL (500 capsules/μL), were irradiated by UV light for different time-intervals. The UV power output was measured using a UV light meter with a peak sensitivity of 365 nm (LUYOR, UV 340B, China). The power output of the lamp (LUYOR-365, China) at 365 nm was ca. 35 mW/cm^2. After UV irradiation and different releasing time-intervals, sample solutions were centrifuged at 500 rpm to precipitate the residual capsules, and the fluorescence of the released TMR-D or DOX-D in the supernatant solution was measured by a Cary Eclipse fluorescence spectrophotometer (Varian, Inc.). Before the measuring of the DOX-D fluorescence, 5 μL of hydrochloric acid was added into the DOX-D supernatant solution to release the DOX from the dextran. The catalytic activity of the released MP-11 was assayed by incubating 10 μL of supernatant solution with 100 μL of HEPES buffer solution, 10 mM, pH 7, containing 500 mM NaCl, in the presence of 100 μM Amplex UltraRed and 0.1 mM H_2O_2.

pH-Induced Unlocking of the i-Motif-Based Microcapsules and the Release of Loads. The pH-responsive microcapsule solution, 40 μL (500 capsules/μL), was treated with 1 μL of 10% acetic acid or 15% ammonium hydroxide to adjust pH. After different incubation time-intervals, the capsule solution was centrifuged at 500 rpm for 20 min to precipitate the residual capsules. The fluorescence intensity of the released CdSe/ZnS QDs in the supernatant solutions was measured by a Cary Eclipse Fluorescence Spectrophotometer (Varian, Inc.).

Cell Culture. Malignant breast epithelial cells (MDA-MB-231) were grown at 37 °C under 5% CO_2 using a RPMI 1640 medium supplemented with 10% Fetal Calf Serum, L-glutamine, and antibiotics containing penicillin, streptomycin, and amphotericin B (Biological Industries). Normal breast cells (MCF-10A) were grown in a medium consisting of 1:1 mixture of Dulbecco's modified Eagle's medium and Ham's F12 medium supplemented with 5% horse bovine serum, 20 ng/mL epidermal growth factor, 0.1 μg/ml cholera toxin (CT), 10 μg/mL insulin, 500 ng/mL hydrocortisone, and 1 unit/mL penicillin/streptomycin.

Uptake into Cells of the Microcapsules. Normal breast cells (MCF-10A) or malignant breast epithelial cells (MDA-MB-231) were planted on glass-bottomed Petri-dish and incubated with 7.5 × 10^5 capsules/mL of CdSe/ZnS QDs-loaded capsules in the growth medium for 6 h. Then, the cells were intensively washed with DMEM-Hepes, and the fluorescence of QDs was measured by epi-fluorescence microscopy (Nikon TE2000 microscope) equipped with opti-grid. Image analysis was performed using ImageJ.

Cell Viability. MCF-10A or MDA-MB-231 breast epithelial cells were seeded on 24-well plates and allowed to grow overnight to reach cell densities of 1.8 × 10^5 cells/well. The resulting cells were treated with DOX-D-loaded microcapsules or with empty microcapsules for a time-interval of 6 h (addition of 33 μL of the microcapsules, 2.5 × 10^4 capsules/mL). Following intensive washing, the cells were exposed to UV light, λ = 365 nm, for 5 min, and subsequently were incubated for 24 h in the growth medium at pH 6. The cell viability was determined with the fluorescent redox probe, Alamar Blue. The fluorescence of Alamar Blue was recorded on a plate-reader (Tecan Safire) after 1 h of incubation at 37 °C (λ_{ex} = 560 nm; λ_{em} = 590 nm).

■ ASSOCIATED CONTENT

Supporting Information

The Supporting Information is available free of charge on the ACS Publications website at DOI: 10.1021/jacs.6b04773.

SEM images, confocal images of microcapsules calibration curves, and cell cytotoxicity results are provided (PDF)

Movie showing the decomposition of the shell of the microcapsules and the release of the respective load is provided (AVI)

■ AUTHOR INFORMATION

Corresponding Author

*willnea@vms.huji.ac.il

Author Contributions

F.H. and W.C.L. contributed equally.

Notes

The authors declare no competing financial interest.

■ ACKNOWLEDGMENTS

The research is supported by the Minerva Center for Biohybrid Complex Systems and by the Israel Science Foundation.

■ REFERENCES

(1) Ochs, M.; Carregal-Romero, S.; Rejman, J.; Braeckmans, K.; De Smedt, S. C.; Parak, W. J. *Angew. Chem., Int. Ed.* **2013**, *52*, 695−699.
(2) Peyratout, C. S.; Dahne, L. *Angew. Chem., Int. Ed.* **2004**, *43*, 3762−3783.
(3) Shi, J. F.; Jiang, Y. J.; Wang, X. L.; Wu, H.; Yang, D.; Pan, F. S.; Su, Y. L.; Jiang, Z. Y. *Chem. Soc. Rev.* **2014**, *43*, 5192−5210.
(4) Skirtach, A. G.; Yashchenok, A. M.; Möhwald, H. *Chem. Commun.* **2011**, *47*, 12736−12746.
(5) Tong, W. J.; Song, X. X.; Gao, C. Y. *Chem. Soc. Rev.* **2012**, *41*, 6103−6124.
(6) Volodkin, D. V.; Petrov, A. I.; Prevot, M.; Sukhorukov, G. B. *Langmuir* **2004**, *20*, 3398−3406.
(7) Hartmann, R.; Weidenbach, M.; Neubauer, M.; Fery, A.; Parak, W. J. *Angew. Chem., Int. Ed.* **2015**, *54*, 1365−1368.
(8) Antipov, A. A.; Sukhorukov, G. B.; Leporatti, S.; Radtchenko, I. L.; Donath, E.; Möhwald, H. *Colloids Surf., A* **2002**, *198*, 535−541.
(9) Donath, E.; Sukhorukov, G. B.; Caruso, F.; Davis, S. A.; Möhwald, H. *Angew. Chem., Int. Ed.* **1998**, *37*, 2201−2205.
(10) Lvov, Y.; Decher, G.; Möhwald, H. *Langmuir* **1993**, *9*, 481−486.

(11) Zhu, Y.; Tong, W. J.; Gao, C. Y. *Soft Matter* **2011**, *7*, 5805–5815.
(12) Connal, L. A.; Kinnane, C. R.; Zelikin, A. N.; Caruso, F. *Chem. Mater.* **2009**, *21*, 576–578.
(13) Ochs, C. J.; Such, G. K.; Yan, Y.; van Koeverden, M. P.; Caruso, F. *ACS Nano* **2010**, *4*, 1653–1663.
(14) Becker, A. L.; Zelikin, A. N.; Johnston, A. P. R.; Caruso, F. *Langmuir* **2009**, *25*, 14079–14085.
(15) Skirtach, A. G.; Javier, A. M.; Kreft, O.; Kohler, K.; Alberola, A. P.; Möhwald, H.; Parak, W. J.; Sukhorukov, G. B. *Angew. Chem., Int. Ed.* **2006**, *45*, 4612–4617.
(16) Angelatos, A. S.; Radt, B.; Caruso, F. *J. Phys. Chem. B* **2005**, *109*, 3071–3076.
(17) Skirtach, A. G.; Dejugnat, C.; Braun, D.; Susha, A. S.; Rogach, A. L.; Parak, W. J.; Möhwald, H.; Sukhorukov, G. B. *Nano Lett.* **2005**, *5*, 1371–1377.
(18) Carregal-Romero, S.; Guardia, P.; Yu, X.; Hartmann, R.; Pellegrino, T.; Parak, W. J. *Nanoscale* **2015**, *7*, 570–576.
(19) De Geest, B. G.; Skirtach, A. G.; Mamedov, A. A.; Antipov, A. A.; Kotov, N. A.; De Smedt, S. C.; Sukhorukov, G. B. *Small* **2007**, *3*, 804–808.
(20) Kolesnikova, T. A.; Gorin, D. A.; Fernandes, P.; Kessel, S.; Khomutov, G. B.; Fery, A.; Shchukin, D. C.; Möhwald, H. *Adv. Funct. Mater.* **2010**, *20*, 1189–1195.
(21) Pavlov, A. M.; Saez, V.; Cobley, A.; Graves, J.; Sukhorukov, G. B.; Mason, T. J. *Soft Matter* **2011**, *7*, 4341–4347.
(22) del Mercato, L. L.; Gonzalez, E.; Abbasi, A. Z.; Parak, W. J.; Puntes, V. *J. Mater. Chem.* **2011**, *21*, 11468–11471.
(23) Shiratori, S. S.; Rubner, M. F. *Macromolecules* **2000**, *33*, 4213–4219.
(24) Lutkenhaus, J. L.; McEnnis, K.; Hammond, P. T. *Macromolecules* **2007**, *40*, 8367–8373.
(25) Hartmann, L.; Bedard, M.; Borner, H. G.; Möhwald, H.; Sukhorukov, G. B.; Antonietti, M. *Soft Matter* **2008**, *4*, 534–539.
(26) Levy, T.; Dejugnat, C.; Sukhorukov, G. B. *Adv. Funct. Mater.* **2008**, *18*, 1586–1594.
(27) Zelikin, A. N.; Li, Q.; Caruso, F. *Angew. Chem., Int. Ed.* **2006**, *45*, 7743–7745.
(28) De Geest, B. G.; Vandenbroucke, R. E.; Guenther, A. M.; Sukhorukov, G. B.; Hennink, W. E.; Sanders, N. N.; Demeester, J.; De Smedt, S. C. *Adv. Mater.* **2006**, *18*, 1005–1009.
(29) Rivera-Gil, P.; De Koker, S.; De Geest, B. G.; Parak, W. J. *Nano Lett.* **2009**, *9*, 4398–4402.
(30) de Villiers, M. M.; Lvov, Y. M. *Adv. Drug Delivery Rev.* **2011**, *63*, 699–700.
(31) Shchukina, E. M.; Shchukin, D. G. *Adv. Drug Delivery Rev.* **2011**, *63*, 837–846.
(32) Becker, A. L.; Orlotti, N. I.; Folini, M.; Cavalieri, F.; Zelikin, A. N.; Johnston, A. P. R.; Zaffaroni, N.; Caruso, F. *ACS Nano* **2011**, *5*, 1335–1344.
(33) Ai, H. *Adv. Drug Delivery Rev.* **2011**, *63*, 772–788.
(34) Reibetanz, U.; Chen, M. H. A.; Mutukumaraswamy, S.; Liaw, Z. Y.; Oh, B. H. L.; Donath, E.; Neu, B. *J. Biomater. Sci., Polym. Ed.* **2011**, *22*, 1845–1859.
(35) del Mercato, L. L.; Abbasi, A. Z.; Ochs, M.; Parak, W. J. *ACS Nano* **2011**, *5*, 9668–9674.
(36) Balabushevich, N. G.; Sukhorukov, G. B.; Larionova, N. I. *Macromol. Rapid Commun.* **2005**, *26*, 1168–1172.
(37) Stein, E. W.; Volodkin, D. V.; McShane, M. J.; Sukhorukov, G. B. *Biomacromolecules* **2006**, *7*, 710–719.
(38) Johnston, A. P. R.; Mitomo, H.; Read, E. S.; Caruso, F. *Langmuir* **2006**, *22*, 3251–3258.
(39) Fujii, A.; Maruyama, T.; Ohmukai, Y.; Kamio, E.; Sotani, T.; Matsuyama, H. *Colloids Surf., A* **2010**, *356*, 126–133.
(40) Johnston, A. P. R.; Lee, L.; Wang, Y. J.; Caruso, F. *Small* **2009**, *5*, 1418–1421.
(41) Liao, W. C.; Lu, C. H.; Hartmann, R.; Wang, F. A.; Sohn, Y. S.; Parak, W. J.; Willner, I. *ACS Nano* **2015**, *9*, 9078–9086.
(42) Bochet, C. G. *J. Chem. Soc., Perkin Trans. 1* **2002**, 125–142.
(43) Pelliccioli, A. P.; Wirz, J. *Photochem. Photobiol. Sci.* **2002**, *1*, 441–458.
(44) Pirrung, M. C.; Lee, Y. R.; Park, K.; Springer, J. B. *J. Org. Chem.* **1999**, *64*, 5042–5047.
(45) Zhao, J.; Gover, T. D.; Muralidharan, S.; Auston, D. A.; Weinreich, D.; Kao, J. P. Y. *Biochemistry* **2006**, *45*, 4915–4926.
(46) Huang, F. J.; Xu, H. G.; Tan, W. H.; Liang, H. J. *ACS Nano* **2014**, *8*, 6849–6855.
(47) Han, X. J.; Critchley, K.; Zhang, L. X.; Pradeep, S. N. D.; Bushby, R. J.; Evans, S. D. *Langmuir* **2007**, *23*, 1354–1358.
(48) Han, X. J.; Pradeep, S. N. D.; Critchley, K.; Sheikh, K.; Bushby, R. J.; Evans, S. D. *Chem. - Eur. J.* **2007**, *13*, 7957–7964.
(49) Huang, F. J.; Zhou, X.; Yao, D. B.; Xiao, S. Y.; Liang, H. J. *Small* **2015**, *11*, 5800–5806.
(50) Zhang, Z. X.; Balogh, D.; Wang, F. A.; Sung, S. Y.; Nechushtai, R.; Willner, I. *ACS Nano* **2013**, *7*, 8455–8468.
(51) Aujard, I.; Benbrahim, C.; Gouget, M.; Ruel, O.; Baudin, J. B.; Neveu, P.; Jullien, L. *Chem. - Eur. J.* **2006**, *12*, 6865–6879.

DOI: 10.1021/jacs.6b04773
J. Am. Chem. Soc. 2016, 138, 8936–8945